

Bioactive Sesquiterpenes from the Edible Mushroom *Flammulina velutipes* and Their Biosynthetic Pathway Confirmed by Genome Analysis and Chemical Evidence

Qiaoqiao Tao,^{†,‡,#} Ke Ma,^{†,#} Yanlong Yang,^{†,#} Kai Wang,^{†,‡} Baosong Chen,^{†,‡} Ying Huang,[§] Junjie Han,[†] Li Bao,[†] Xiao-Bin Liu,^{||} Zhuliang Yang,^{||} Wen-Bing Yin,^{†,‡} and Hongwei Liu^{*,†,‡}

[†]State Key Laboratory of Mycology, Institute of Microbiology, Chinese Academy of Sciences, Beijing 100101, People's Republic of China

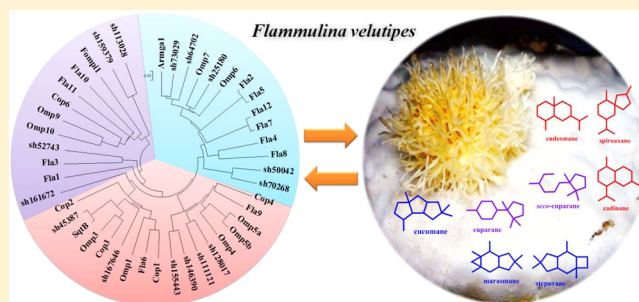
[‡]Savaid Medical School, University of Chinese Academy of Sciences, Beijing 100049, People's Republic of China

[§]State Key Laboratory of Microbial Resources, Institute of Microbiology, Chinese Academy of Sciences, Beijing 100101, People's Republic of China

^{||}Key Laboratory for Plant Diversity and Biogeography of East Asia, Kunming Institute of Botany, Chinese Academy of Sciences, Kunming 650201, People's Republic of China

Supporting Information

ABSTRACT: Twelve putative sesquiterpene synthases genes were found in clades along with enzymes with 1,6-, 1,10-, and 1,11-cyclase activities in the genome of *Flammulina velutipes*. Chemistry investigation of *F. velutipes* led to the identification of two *seco*-cuparane sesquiterpenes, flammufuranone A (1) and B (2); 13 new sesquiterpenes with nor-eudesmane, spiroaxane, cadinane, and cuparane skeletons (3–14, 16); as well as two new ergosterol derivatives (17 and 18). Sesquiterpenes (3–14) derived from 1,10-cyclizing enzyme were first reported from this mushroom. The absolute configurations in 1 (3*R*,7*S*) and 2 (3*R*,7*R*) were assigned by electronic circular dichroism (ECD) calculation. The absolute configuration in 3 was confirmed by X-ray diffraction analysis. The absolute configurations in the 1,2-diol moiety of 13, and in the 1,3-diol moiety of 17 and 18 were determined using Snatzke's method. Among these compounds, 3, 5, 13, and 14 were found to inhibit the HMG-CoA reductase with IC₅₀ of 114.7, 77.6, 55.5, and 87.1 μM, respectively. Compounds 5, 6, 7, 10, 13, and 14 showed DPP-4 inhibitory activity with IC₅₀ of 75.9, 83.7, 70.9, 79.7, 80.5, and 74.8 μM, respectively. The biosynthesis for sesquiterpenes in *F. velutipes* was also discussed.



INTRODUCTION

Chemistry of various sesquiterpenes produced by higher plants and fungi continues to attract our attention due to their diverse chemical skeletons, interesting bioactivities, and complicated biosynthesis mechanism.^{1–3} Mushroom is defined as a specific group of fungi with the most conspicuous structure of fruiting body as reproductive organ. To protect the fruiting body from the attack of other organism, mushrooms have developed complex chemical defense mechanism and produced various secondary metabolites as chemical weapons.⁴ Sesquiterpenes from mushrooms have been recognized as not only the chemical defense molecules,⁵ but also the leading compounds for new drug development due to their diverse pharmacological activities.^{6–8} In our early chemical assessment on mushroom *Flammulina velutipes*, we identified 25 new bioactive sesquiterpenes including flammulipenoids with antibacterial activity,⁹ enokipodins with antifungal activity against *Aspergillus fumigatus*,¹⁰ and flammulinolides with strong cytotoxicity against KB cell line.¹¹ To link the sesquiterpene synthase genes with their

corresponding sesquiterpene skeletons in the genomes of basidiomycetes, a predictive framework has been developed by Schmidt-Dannert group based on multiple sequence alignments and phylogenetic analyses.¹² The predictive framework method has been as a roadmap for the discovery of specific sesquiterpene synthases from basidiomycota and has been verified by successful identification and characterization of 1,6-, 1,10-, and 1,11-cyclizing sesquiterpene synthases in *Stereum hirsutum*.¹³ Inspired by these findings, we identified 12 putative sesquiterpene synthases genes totally, designated as Fla 1–12, from the genome of *F. velutipes* by BLAST searches using 19 identified previously fungal sesquiterpene synthases from *Coprinus cinereus*, *Omphalotus olearius*, and *S. hirsutum* (Supporting Information, Table S1).^{12–14} Phylogenetic analyses indicated Fla6 in Clade I; Fla9 in Clade II; Fla2, Fla4, Fla5, Fla 7, Fla 8, Fla12 in Clade III; and Fla1, Fla3, Fla10, Fla11 in

Received: August 14, 2016

Published: September 29, 2016

Clade IV (Figure 1). The sesquiterpenes derived from sesquiterpene synthases in Clade III and Clade IV were

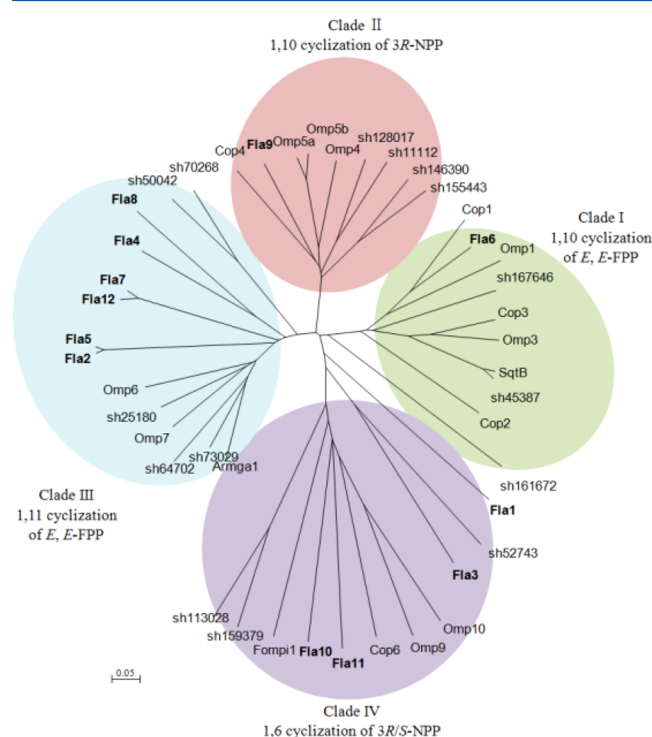


Figure 1. Phylogenetic analysis of sesquiterpene synthase homologues.

reported in our early research on *F. velutipes*.^{9–11} The sesquiterpenes catalyzed by sesquiterpene synthases in Clade I and Clade II from 1,10-cyclization mechanisms have not been discovered in this mushroom.

To discover new sesquiterpenes derived from 1,10-cyclization, six strains of *F. velutipes* deposited in our group were fermented, and the corresponding culture extracts were analyzed by HPLC technique. As a result, the ethyl acetate extract from a wild strain of *F. velutipes* collected in Yunnan province of China showed rich sesquiterpenes which are different from our early reports. Chemical investigation on the culture extract of this strain led to the isolation of 15 new sesquiterpenes with various skeletons, including nor-eudesmane, spiroaxane, cadinane, cuparane, and *seco*-cuparane. Herein, we report the isolation, structural elucidation, bioactivities, and the insight into the plausible biogenesis of these sesquiterpenes.

RESULTS AND DISCUSSION

The fungus *F. velutipes* was cultured by solid-state fermentation method with rice as medium for 40 days and extracted three times with EtOAc. The resulting organic extract (16.2 g) was fractionated by silica gel chromatography, Sephadex LH-20 column chromatography, and reversed-phase HPLC to afford 16 sesquiterpenoids (1–16) and two new ergosterol derivatives (17,18).

Flammufuranone A (1) was isolated as colorless oil. It gave a $[M+H]^+$ ion in the HRTOFMS at m/z 279.1227, indicating a molecular formula of $C_{15}H_{18}O_5$ (7 degrees of unsaturation). The 1H and ^{13}C NMR data (Table 1) suggested the presence of 15 carbons resonances. Eight of 15 carbons were identified as hydrogen-bearing carbons in a further HSQC experiment, four

Table 1. 1H and ^{13}C NMR Data for Compounds 1 and 2 in CD_3OD

pos.	1		2	
	δ_C	δ_H mult. (J in Hz)	δ_C	δ_H mult. (J in Hz)
1	171.8		171.6	
2	41.4	2.82 o	41.7	2.87 o
3	89.2		88.9	
4	208.0		207.9	
5	103.9	5.65 s	103.9	5.60 s
6	193.8		193.6	
7	55.2		55.1	
8	165.8	7.70 d (5.9)	165.9	7.77 d (5.9)
9	131.5	6.25 d (5.9)	131.5	6.26 d (5.9)
10	214.2		214.0	
11	52.0		51.7	
12	20.8	1.16 s	20.6	1.19 s
13	24.4	1.06 s	24.9	1.07 s
14	22.6	1.42 s	22.7	1.40 s
15	22.6	1.41 s	22.6	1.42 s

methyls (δ_C 24.4, 22.6, 22.6, and 20.8), one methylene (δ_C 41.4), and three olefinic methines (δ_C 165.8, 131.5, and 103.9). The seven quaternary carbons were revealed as two carbonyl carbons (δ_C 214.2 and 208.0), one carboxylic carbon (δ_C 171.8), one olefinic carbon (δ_C 193.8), and two sp^3 -hybridized quaternary carbons (δ_C 89.2, 55.2, and 52.0). In the HMBC spectrum of 1, the correlations from H_3 -12 to C-7, C-10, C-11, and C-13, and from H-9 to C-7, C-8, C-10, and C-11 furnished an α,β -unsaturated cyclopentanone moiety (Figure 2). Further inspection of the HMBC correlations from H-8 to C-6, C-7, C-11, and C-14, from H_3 -14 to C-6, C-7, C-8, and C-11, from H-5 to C-3, C-4, C-6, and C-7, from H_2 -2 to C-1, C-3, and C-15, and from H_3 -15 to C-2, C-3, and C-4 established the planar structure and satisfied the unsaturation requirement (Figure 3).

Flammufuranone B (2), an isomer of 1, was obtained as colorless oil. Detailed interpretation of its HRTOFMS and NMR data confirmed that it had the same planar structure as that of 1. There were two stereogenic centers at C-3 and C-7 in 1 and 2, which led to four possible isomers (1a and 1b; 2a and 2b). In the CD spectrum of 1, one positive Cotton effect at 295 nm and two negative Cotton effects at 228 and 340 nm were observed. Compound 2 showed one positive Cotton effect at 263 nm and two negative Cotton effects at 216 and 300 nm, respectively. The difference in the CD spectrum between 1 and 2 demonstrated that they were a pair of epimers. To determine the absolute configurations in 1 and 2, ECD calculation method by time-dependent density functional theory (TDDFT) at the B3LYP/6-311G(d,p) level was applied.¹⁵ By comparison of the experimental and simulated ECD curves (Figure 4), the absolute configurations at C-3 and C-7 were assigned as 3*R*,7*S* in 1 and 3*R*,7*R* in 2, respectively.

Flammuspironone A (3) was isolated as colorless needles. The HRTOFMS data of 3 indicated a molecular formula of $C_{15}H_{24}O_4$ (4 degrees of unsaturation). Analysis of its 1D NMR data (Table 2 and Table 3) and HSQC revealed four methyls (δ_C 28.7, 27.4, 16.3, and 10.2), two methylenes (δ_C 46.1 and 42.0), four methines (δ_C 76.5, 69.3, 54.3, and 32.7), two quaternary carbons (δ_C 75.2 and 54.1), two olefinic carbons (δ_C 161.2 and 144.7), and a carbonyl carbons (δ_C 211.1). The 1H - 1H COSY correlations of H-6/H-7/H-8/H-9/H-10/ H_3 -15 together with HMBC correlations from H_3 -15 to C-1, from H-10 to C-5, from H-5 to C-2, C-3, and C-4, from H-

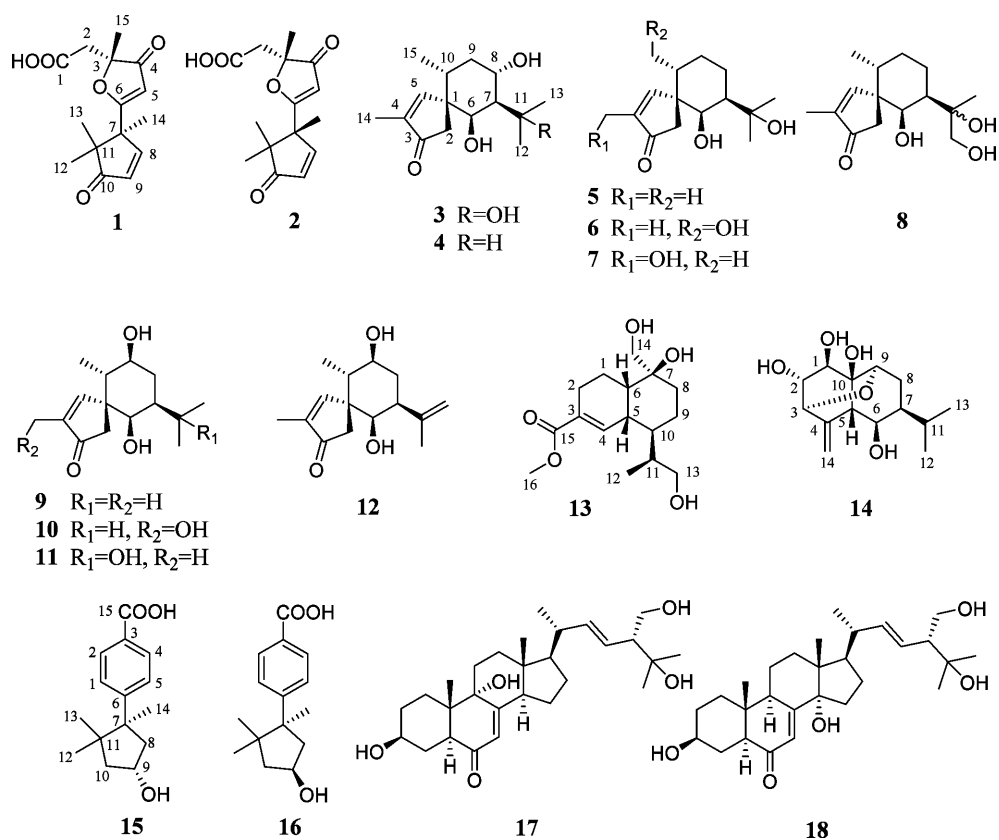
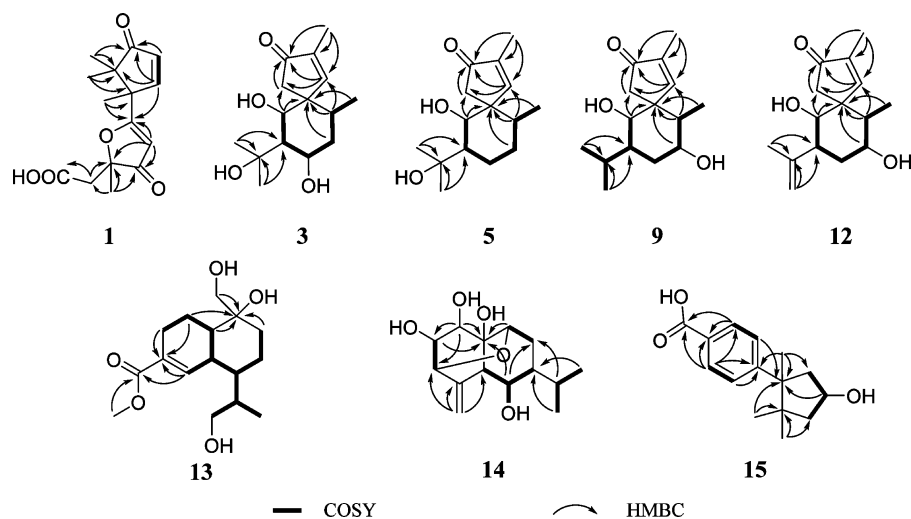


Figure 2. Structures of compounds 1–18.

Figure 3. Key ¹H–¹H COSY and HMBC correlations of 1, 3, 5, 9, and 12–15.

6 to C-1 and C-2, and from H₃-14 to C-3, C-4, and C-5 confirmed the structural moiety of 3,6-dimethylspiro[4.5]dec-3-en-2-one. Finally, the substitution of an oxygenated isopropyl group at C-7 was supported by the HMBC correlations from H₃-12 to C-7, C-11, and C-13 (Figure 3). The relative configuration of 3 was determined as shown by NOESY correlations of H-5 with H-6, H-7 with H₃-15, as well as H-10 with H-2a (δ_{H} 2.23) and H-8 (Supporting Information, Figure S3). The absolute configuration of compound 3 was established as 1*S*,6*R*,7*R*,8*S*,10*R* by a single X-ray crystallography analysis (Figure 5) with the Flack parameter value close to zero [−0.02 (12)].

The molecular formula of flammuspiron B (4) was determined to be C₁₅H₂₄O₃ on the basis of the [M+H]⁺ ion in the HRTOFMS at *m/z* 253.1798. The ¹H and ¹³C NMR data of 4 were similar to those of 3, except for an additional methine ($\delta_{\text{H}}/\delta_{\text{C}}$ 2.13/28.9) replacing the oxygenated quaternary carbon (δ_{C} 75.2). The HMBC correlations from H-11 to C-6, C-7, C-8, C-12, and C-13 confirmed the location of an isopropyl group at C-7 (Supporting Information, Figure S2). Similar NOE correlations and the same positive Cotton effect at 320 nm between 3 and 4 revealed the absolute configuration of 4 as 1*S*,6*R*,7*R*,8*S*,10*R* (Supporting Information, Figure S6).

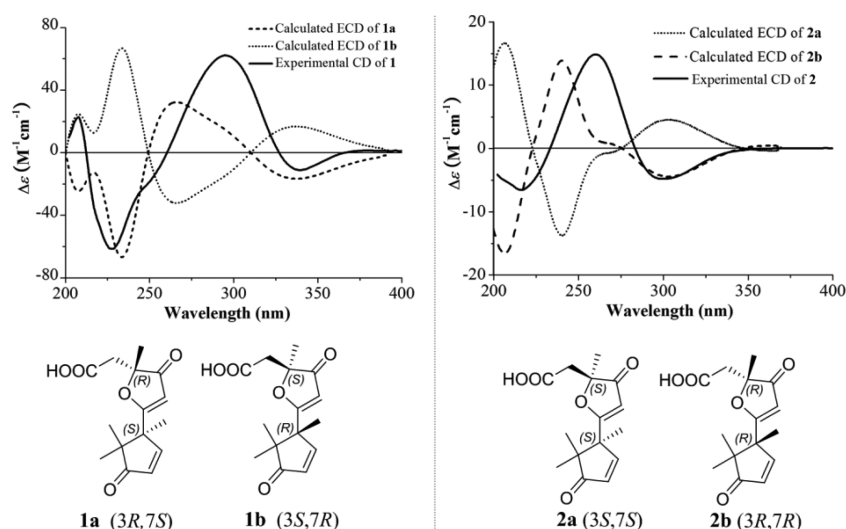


Figure 4. B3LYP/6-311G (d,p)-calculated ECD spectrum of (3R,7S)-1a and (3S,7S)-2a and experimental ECD spectrum of 1 and 2.

Table 2. ¹H NMR Data for Compounds 3–8 in CD₃OD

pos.	δ_{H} mult. (J in Hz)						
	3	4	5	6	7	8	
1							
2	2.44 d (19.3)	2.45 d (19.3)	2.47 d (19.3)	2.57 o	2.54 d (19.3)	2.49 d (19.3)	
	2.23 d (19.3)	2.22 d (19.3)	2.27 d (19.3)	2.51 o	2.33 d (19.3)	2.27 d (19.3)	
3							
4							
5	7.48 d (1.0)	7.43 d (1.2)	7.44 d (1.3)	7.47 d (1.1)	7.57 s	7.43 d (1.1)	
6	3.61 d (1.8)	3.57 d (1.9)	3.80 s	3.72 s	3.84 s	3.78 s	
7	1.76 o	1.52 m	1.67 o	1.66 m	1.71 o	1.92 m	
8	4.26 td (11.1, 4.8)	3.99 dt (11.1, 4.8)	1.81 m	1.82 m	1.82 o	1.81 m	
						1.71 o	
9	1.86 m	1.88 m	1.69 o	1.96 m	1.74 o	1.69 o	
	1.45 o	1.34 m	1.37 m	1.36 m	1.40 m	1.37 m	
10	2.17 m	2.16 o	2.08 m	2.11 m	2.12 m	2.09 m	
11		2.13 o					
12	1.44 o	1.07 d (7.1)	1.24 s	1.25 s	1.25 s	1.24 s	
13	1.23 s	1.04 d (7.1)	1.28 s	1.28 s	1.29 s	3.50 d (11.0)	
						3.39 d (11.0)	
14	1.78 o	1.77 d (1.2)	1.77 d (1.3)	1.75 d (1.1)	4.27 d (15.2)	1.77 d (1.1)	
					4.23 d (15.2)		
15	0.70 d (6.9)	0.69 d (6.9)	0.67 d (6.9)	3.35 o	0.71 d (6.9)	0.66 d (6.8)	
				3.13 dd (11.0, 7.6)			

The molecular formula of flammuspironone C (**5**) was determined to be C₁₅H₂₄O₃ based on the HRTOFMS [M + H]⁺ ion at *m/z* 253.1796. The 1D and 2D NMR data of **5** was similar to those of **3** revealed that they shared the similar structure. Compound **5** was different from **3** by replacing the oxygenated methine with a methylene group at C-8, which was supported by the ¹H–¹H COSY and HMBC correlations from H-8 (δ_{H} 1.81) to C-6, C-7, C-9, C-10, and C-11. The absolute configuration of **5** was further determined as 1S,6R,7R,10R by comparing the CD spectrum of **5** with that of **3** (Supporting Information, Figure S6).

Flammuspirones D (**6**), E (**7**), and F (**8**) were assigned to have the same molecular formula of C₁₅H₂₄O₄ according to their HRTOFMS data at *m/z* 269.1747 ([M + H]⁺, **6**), 291.1568 ([M + Na]⁺, **7**), and 269.1747 ([M + H]⁺, **8**). The NMR data of **6**, **7**, and **8** showed much similarity with those of **5** except that

one methylene bearing an oxygen atom took the place of one methyl group in **6**, **7**, and **8**. The structure of **6**, **7**, and **8** were finally determined as described by detailed analysis of their ¹H–¹H COSY and HMBC spectra, respectively. The same positive Cotton effects deriving from *n*– π^* transitions in α,β -unsaturated ketone moiety at 320 nm allowed the unambiguous assignment of the absolute configuration of 1R,6R,7R,10R in **6**, **7**, **8**, respectively. The absolute configuration at C-11 in **8** was left unsolved in this work.

Flammuspironone G (**9**) was assigned a molecular formula of C₁₅H₂₄O₃ through the interpretation of HRTOFMS data ([M + Na]⁺, *m/z* 275.1617). The 1D and 2D NMR data suggested that compound **9** had the same skeleton as that of **5**. Interpretation of COSY and HMBC spectroscopic data provided evidence of the substitution of a hydroxyl group at C-9 (Figure 3). NOE correlations from H-5 to H-6, H-7, H-9,

Table 3. ^{13}C NMR Data for Compounds 3–13 in CD_3OD and 14 in $\text{DMSO}-d_6$

pos.	δ_{C}												
	3	4	5	6	7	8	9	10	11	12	13	14	
1	54.1	54.0	53.8	52.4	54.2	53.8	54.5	54.8	54.3	54.4	21.5	78.9	
2	46.1	46.2	46.6	46.8	47.5	46.8	47.0	47.9	46.5	47.1	25.3	77.3	
3	211.1	211.4	211.5	211.2	209.7	211.5	211.3	209.5	211.0	211.2	130.5	76.1	
4	144.7	144.4	144.4	144.0	148.6	144.4	144.3	148.4	144.6	144.5	140.0	145.4	
5	161.2	161.8	161.9	161.6	161.1	161.9	162.2	161.4	161.6	161.8	39.4	40.0	
6	76.5	77.5	76.1	76.6	75.6	75.5	74.8	74.7	75.2	75.0	48.1	72.5	
7	54.3	50.7	47.2	47.2	47.2	44.2	45.0	45.0	45.6	44.5	72.9	37.5	
8	69.3	68.7	21.6	21.0	21.6	21.6	34.4	34.4	30.9	34.3	34.5	25.9	
9	42.0	42.4	32.2	27.3	32.3	32.3	73.5	73.5	73.5	73.3	21.3	72.4	
10	32.7	32.8	33.6	41.4	33.7	33.7	41.2	41.2	41.1	41.3	40.7	70.9	
11	75.2	28.9	73.8	73.8	73.8	75.7	29.9	30.0	73.6	147.1	34.2	27.9	
12	27.4	20.6	28.4	28.4	28.5	24.4	21.1	21.1	28.5	22.5	9.2	20.7	
13	28.7	21.3	28.8	28.8	28.8	68.2	21.4	21.4	28.8	111.9	65.4	20.8	
14	10.2	10.1	10.1	10.2	57.2	10.1	10.1	57.0	10.1	10.1	61.8	110.4	
15	16.3	16.4	16.3	64.9	16.3	16.3	12.1	12.1	12.1	12.1	168.2		
16											50.7		

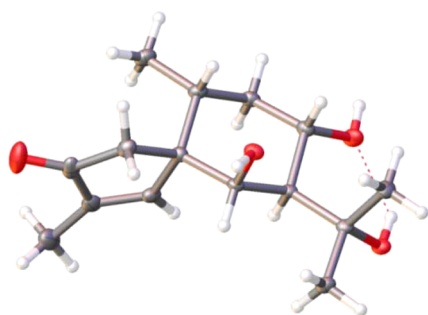


Figure 5. Thermal ellipsoid representation (drawn at the 50% probability level) of **3**.

and $\text{H}_3\text{-15}$ together with same Cotton effect between **3** and **9** led to the absolute configuration assignment of $1R,6R,7S,9S,10S$ for **9**.

Flammuspirones **H** (**10**) and **I** (**11**) were assigned as hydroxyl-substituted derivatives of **9** based on their HRTOFMS data and NMR data (Tables 3 and 4). The low-field shift of C-14 ($\Delta\delta_{\text{C}} = 46.9$) in **10** and C-11 ($\Delta\delta_{\text{C}} = 43.6$) in **11** revealed the location of additional hydroxyl group, respectively. In combination with the relative configuration determined by NOE correlations, the positive Cotton effect at 300 nm in **10** and **11** implied the absolute configuration of **10** to be $1R,6R,7S,9S,10S$ and the absolute configuration of **11** to be $1R,6R,7R,9S,10S$.

Flammuspirones **J** (**12**) was isolated as colorless needles. Its molecular formula of $\text{C}_{15}\text{H}_{22}\text{O}_3$ was assigned by the $[\text{M}+\text{H}]^+$ ion at m/z 251.1642 in the HRTOFMS. The ^1H and ^{13}C NMR data of **12** was much similar to those of **9** except for the presence of the terminal double bond ($\delta_{\text{H}}/\delta_{\text{C}}$ 4.79 (1H, s) and 4.90 (1H, s)/111.9; δ_{C} 147.1). HMBC correlations from H-13 to C-7, C-11, and C-12, from H-7 to C-11, C-12, and C-13, and from H-12 to C-7, C-11, and C-13 confirmed the structural variations at the side chain (Table 3 and Table 4). A detailed analysis of the NOESY spectrum and the positive Cotton effect at 320 nm assigned the absolute configuration of **12** to be $1R,6R,7S,9S,10S$.

The molecular formula of **13** was determined to be $\text{C}_{16}\text{H}_{26}\text{O}_5$ based on a HRTOFMS $[\text{M}+\text{H}]^+$ ion at m/z 299.1852, requiring 4 degrees of unsaturation. Its ^1H and ^{13}C NMR

indicated the presence of one methyl (δ_{C} 9.2), one oxymethyl (δ_{C} 50.7), four methylenes (δ_{C} 34.5, 25.3, 21.5, and 21.3), two oxymethylenes (δ_{C} 65.4 and 61.8), four methines (δ_{C} 48.1, 40.7, 39.4, and 34.2), one oxygenated sp^3 quaternary carbons (δ_{C} 72.9), two olefinic carbons (δ_{C} 140.0 and 130.5), and one carboxylic carbon (δ_{C} 168.2). Examination of the ^1H - ^1H COSY data together with HMBC correlations from H-1 to C-7 and C-3, from H-4 to C-15, from H-14 to C-6, C-7, and C-8, and from $\text{H}_3\text{-16}$ to C-15 revealed structure of compound **13** as 7,13,14-trihydroxy-4-cadinen-15-oic acid methyl ester (Figure 2). The relative configuration of **13** was assigned by NOE correlations of H-5 with H-6 and $\text{H}_3\text{-12}$, H-4 with H-11, H-9a (δ_{H} 1.30) with H-6 and $\text{H}_3\text{-12}$ and H-9b (δ_{H} 1.56) with H-14 and $\text{H}_2\text{-13}$. The absolute configuration at C-7 in **13** was assigned as $7S$ by applying the Sznatzke's method¹⁶ base on an observed positive Cotton effect at 298 nm in the $\text{Mo}_2(\text{OAc})_4$ -induced CD spectrum (Figure 6). According to the relative configuration assigned, the absolute configuration in **13** was finally solved as $5R,6S,7S,10R,11S$.

Compound **14** was assigned the molecular formula $\text{C}_{14}\text{H}_{22}\text{O}_5$ (4 degrees of unsaturation) by the HRTOFMS ion at m/z 293.1359 for $[\text{M}+\text{Na}]^+$. Examination of the 1D and 2D NMR data indicated the presence of two methyls (δ_{C} 20.7 and 20.8), one methylene (δ_{C} 25.9), three methines (δ_{C} 40.0, 37.5, and 27.9), five oxymethines (δ_{C} 78.9, 77.3, 76.1, 72.5, and 72.4), one oxygenated sp^3 quaternary carbon (δ_{C} 70.9), and two olefinic carbons (δ_{C} 145.4 and 110.4). Extensive analysis of the ^1H - ^1H COSY data together with HMBC correlations from H-15 to C-3, C-4, and C-5, from H-1 to C-2, C-3, and C-10, from H-6 to C-10 and C-8, from H-12 to C-7, C-11, and C-13, from H-11 to C-8, and from H-9 to C-10 revealed a nor-eudesmane skeleton. Further analysis of HMBC correlations from HO-1 (δ_{H} 4.90) to C-1, C-2, and C-10, from HO-2 (δ_{H} 5.00) to C-1, C-2, and C-3, from HO-6 (δ_{H} 5.37) to C-6, and from HO-10 (δ_{H} 5.44) to C-1, C-9, and C-10 indicated the substitution of a hydroxyl group at C-1, C-2, C-6, and C-10, respectively (Figure 2). The final structure of **14** was identified as 1,2,6,10-tetrahydroxy-3,9-epoxy-14-nor-4(14)-eudesmane based on consideration of unsaturation degrees. The relative configuration of **14** was indicated by NOE correlations from H-5 to 10-OH and 1-OH, from H-9 to H-1, 2-OH, and 10-OH, from H-3 to H-14a (δ_{H} 5.02), from H-6 to H-14b (δ_{H} 4.80) and H-7, and from H-

Table 4. ^1H NMR Data for Compounds 9–13 in CD_3OD and 14 in $\text{DMSO}-d_6$

pos.	$\delta_{\text{H,mult.}}$ (J in Hz)					
	9	10	11	12	13	14
1					2.23 m 1.24 o	3.25 dd (3.4 2.8)
2	2.53 d (19.3) 2.30 d (19.3)	2.59 d (19.3) 2.36 d (19.3)	2.54 d (19.3) 2.29 d (19.3)	2.56 d (19.4) 2.30 d (19.4)	2.44 m 2.12 m	3.28 m
3						3.77 d (1.7)
4					7.08 s	
5	7.33 s	7.45 s	7.32 s	7.41 d (1.4)	2.10 m	2.78 m
6	3.45 o	3.50 s	3.77 s	3.45 s	1.41 m	3.93 m
7	1.41 m	1.42 m	1.81 o	2.50 m		1.45 m
8	1.99 m 1.50 m	2.02 o 1.52 m	2.02 o 1.83 o	1.88 o 1.82 m	1.23 o	1.55 o
9	3.44 o	3.46 o	3.50 m	3.52 td (10.9, 4.7)	1.56 m 1.30 m	3.58 s
10	1.92 m	1.96 o	2.00 o	1.95 o	1.50 m	
11	1.68 m	1.69 m			2.18 m	1.64 o
12	0.93 d (6.6)	0.94 d (6.6)	1.28 s	1.77 o	0.84 (7.0)	0.85 d (6.7)
13	0.98 d (6.7)	0.99 d (6.7)	1.30 s	4.90 s 4.79 s	3.46 d (7.2)	0.86 d (6.7)
14	1.76 s	4.26 d (15.2) 4.22 d (15.2)	1.78 s	1.78 o	3.64 d (11.6) 3.53 d (11.6)	5.02 s 4.80 s
15	0.78 d (6.7)	0.82 d (6.7)	0.79 d (6.7)	0.79 d (6.7)		
16					3.71 s	
10-OH						5.44 s
6-OH						5.37 d (6.2)
2-OH						5.00 d (5.9)
1-OH						4.90 d (3.4)

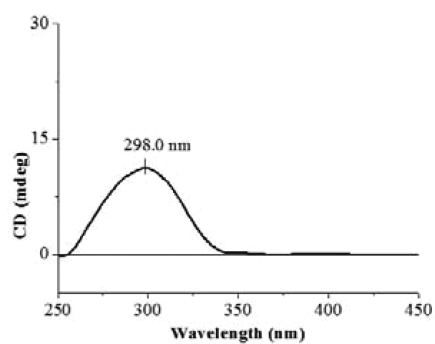


Figure 6. ICD spectrum of Mo-complex of 13 with $\text{Mo}_2(\text{OAc})_4$ and the helicity rule applied.

11 to 6-OH. The absolute configuration at C-5 was determined as 5S by applying olefin rule base on an observed negative Cotton effect at 211 nm in its CD spectrum (Figure 7).¹⁷ Considering the relative configuration determined, the absolute configuration of 14 was assigned as 1R,2R,3S,5S,6R,7S,9R,10S.

Flamvelutpenoids E (15) and F (16) possessed the same molecular formula of $\text{C}_{15}\text{H}_{20}\text{O}_3$, as determined by HRTOFMS data. Examination of their ^1H and ^{13}C NMR data (Table 5) provided evidence of the aromatic cuparane carbon skeleton as comparing with the known compound flamvelutpenoids A.⁹ The HMBC correlations from H-9 to C-7, C-8, C-10, and C-11 and the chemical shift of C-9 (δ_{C} 70.5) determined the substitution of a hydroxyl group at C-9. The relative configuration of 15 and 16 was determined by NOE

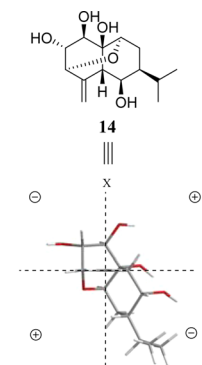
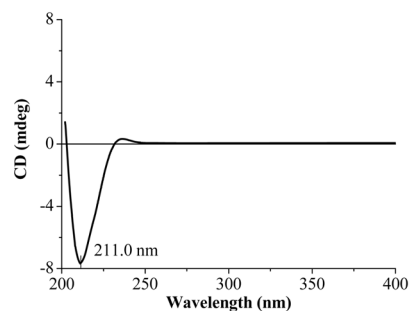
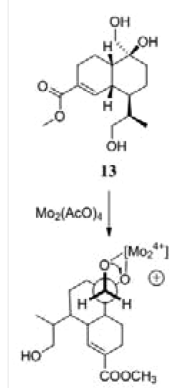


Figure 7. CD spectrum of 14, and the $\pi-\pi^*$ CD rule for olefins applied.

correlations from H₃-14 to H-8a (δ_{H} 1.78), and from H-8b (δ_{H} 3.00) to H-9 in 15, and from H-9 to H₃-14 in 16. Compound 15 was found to have the same planar and relative configuration as that of the enzymatic hydrolysis product of dunnianoside I,¹⁸ whose absolute configuration was determined by analysis of the $\text{Rh}_2(\text{OCOCF}_3)$ -induced CD spectrum. Comparison of the specific rotation value between 15 ($[\alpha]_{\text{D}}^{25}$ -29.0) and the enzymatic hydrolysis product ($[\alpha]_{\text{D}}^{25}$ -29.9) of dunnianoside I indicated that 15 had the same absolute configuration of 7S and 9R as that of dunnianoside I. Compound 15 was reported as a new natural product for the first time. Compound 16 was assigned the same 7S configuration as that of 15 by the negative Cotton effect at about 240 nm. Thus, the absolute configuration of 16 was determined to be 7S,9S.

Table 5. ^1H and ^{13}C NMR Data for Compounds **15** and **16** in CD_3OD

pos.	15		16	
	δ_{C}	$\delta_{\text{Hmult.}}$ (J in Hz)	δ_{C}	$\delta_{\text{Hmult.}}$ (J in Hz)
1	128.1	7.46 d (8.6)	128.1	7.54 d (8.6)
2	130.2	7.93 d (8.6)	130.2	7.94 d (8.6)
3	129.2		129.3	
4	130.2	7.93 d (8.6)	130.2	7.94 d (8.6)
5	128.1	7.46 d (8.6)	128.1	7.54 d (8.6)
6	154.0		153.8	
7	52.1		52.3	
8	48.1	3.00 dd (14.3, 8.5) 1.78 o	48.0	2.57 d (13.1, 6.7) 2.19 o
9	70.5	4.53 m	70.6	4.52 m
10	51.5	2.01 dd (13.7, 8.0) 1.81 o	50.6	2.19 o 1.61 dd (14.0, 4.2)
11	46.0		44.9	
12	24.9	1.19 s	25.1	1.11 s
13	27.0	0.55 s	28.1	0.67 s
14	26.2	1.47 s	25.6	1.31 s
15	170.0		170.0	

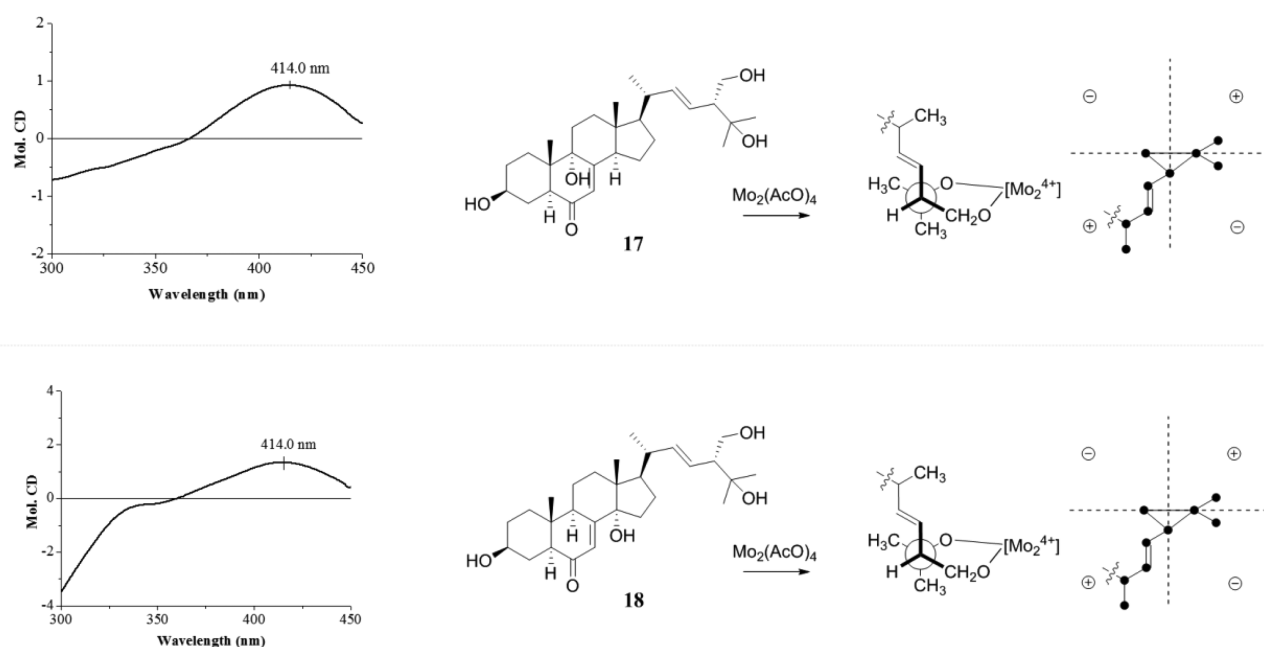
Two new ergosterol derivatives **17** and **18** with the same molecular formula $\text{C}_{28}\text{H}_{44}\text{O}_5$ (based on HRTOFMS) were isolated. The interpretation of 1D and 2D NMR data for **17** and **18** (Supporting Information, Figure S41–44), in combination with the NMR data comparison with known ergosterol derivatives,¹⁹ assigned the structure of **17** and **18** as shown in Figure 2. The absolute configuration at C-24 was determined by sector rule of the CD spectroscopy for the in situ complexation between 1,3-diol and $\text{Mo}_2(\text{OAc})_4$.²⁰ In the $\text{Mo}_2(\text{OAc})_4$ -induced CD spectrum, a positive Cotton effect at 414 nm supported the 24R configuration for **17** and **18** (Figure 8). In the CD spectrum of **17** and **18**, the positive Cotton effects at 330 nm (the exciton coupling of $n-\pi^*$ transition in α,β -unsaturated ketone moiety) confirmed the 5S configuration of **17** and **18** according to the octane rule, respectively.

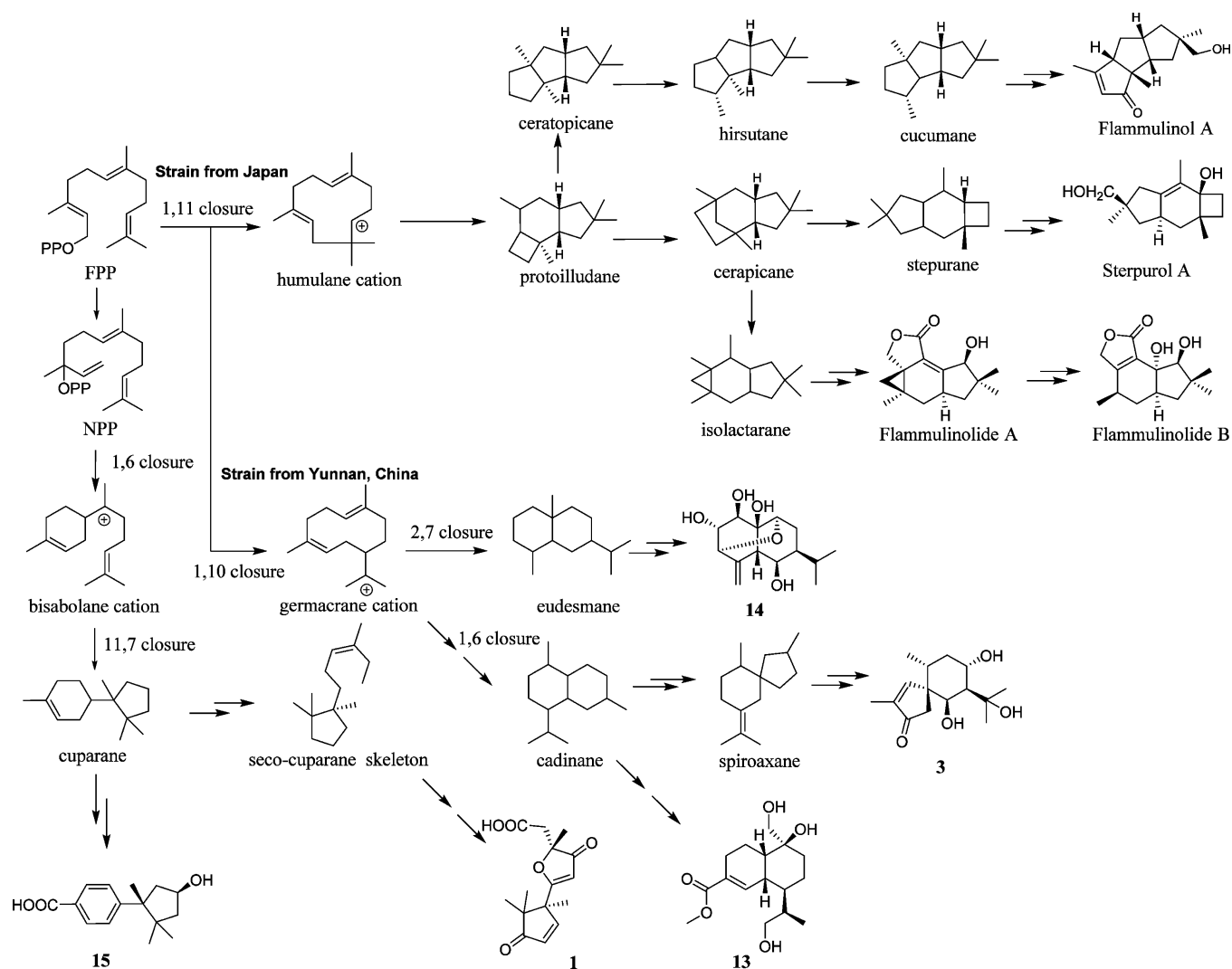
Considering with the relative configuration determined and the biosynthetic origin, the absolute configurations in **17** and **18** were assigned as 3S,5S,9S,10S,13R,14R,17R,20R,24R and 3S,5S,9R,10R,13R,14S,17R,20R,24R.

Edible and medicinal mushrooms were recorded to have beneficial effects for body health through improving hyperglycemic and hyperlipidemic diseases.^{21,22} To search for new natural products with hypoglycemic and hypolipidemic activity, all of the sesquiterpenes (**1–16**) described in this study were evaluated for bioactivities against the HMG-CoA reductase, DPP-4, and aldose reductase. The results are summarized in Table 6. Compounds **3**, **5**, **13**, and **14** showed inhibition on

Table 6. Bioactivities Assay Results of Sesquiterpenes (**1–16**)

compd.	HMG-CoA reductase inhibition (IC_{50} μM)	DPP-4 inhibition (IC_{50} μM)	aldose reductase inhibition (IC_{50} μM)
1	> 150	> 100	> 150
2	> 150	> 100	> 150
3	114.7	> 100	> 150
4	> 150	> 100	> 150
5	77.6	75.9	> 150
6	> 150	83.7	> 150
7	> 150	70.9	> 150
8	> 150	> 100	> 150
9	> 150	> 100	> 150
10	> 150	79.7	> 150
11	> 150	> 100	> 150
12	> 150	> 100	> 150
13	55.5	80.5	> 150
14	87.1	74.8	> 150
15	> 150	> 100	> 150
16	> 150	> 100	> 150
Atorvastatin	26.3		
Sitagliptin		1.4	
Epalrestat			17.5

**Figure 8.** $\text{Mo}_2(\text{OAc})_4$ induced CD spectrum of **17** and **18** when complexed onto molybdenum and the sector rule applied.

Scheme 1. Proposed Biogenetic Pathway for Sesquiterpenes in *F. velutipes*

HMG-CoA reductase with IC_{50} of 114.7, 77.6, 55.5, and 87.1 μM , respectively. In DPP-4 inhibition assay, compounds **5**, **6**, **7**, **10**, **13**, and **14** showed inhibitory activity with IC_{50} values in the range from 70.9 to 83.7 μM . Cytotoxicity against A549, K562, H460, and HepG2 of compounds **1–18** were also examined by using MTT methods.¹¹ None of them showed observable activity against all four tested cell lines at the concentration of 200 μM (cell viability more than 90%).

Basidiomycete fungi are known to produce numerous bioactive sesquiterpenoid metabolites, yet only a few sesquiterpene synthases have been cloned and functionally characterized. To facilitate the discovery of sesquiterpene synthases in basidiomycota, a predictive framework based on multiple sequence alignments and phylogenetic analyses has been developed by Schmidt–Dannert group.¹³ Using this bioinformatic tool, 12 putative sesquiterpene synthases from *F. velutipes* located in clades I–IV were discovered. The Fla6 in Clade I, clustered together with Cop1 and Omp1, likely catalyzes a 1,10-cyclization of (2*E*,6*E*)-FPP to yield cadinane that is the precursor of sesquiterpenoids with nor-eudesmane, spiroaxane, and cadinane skeletons. Alternately, Fla9 of Clade II clustered most closely with cadinane synthases Cop4, Omp4, Omp5a, and Omp5b may also be responsible for the biosynthesis of sesquiterpenoids with nor-eudesmane, spiroax-

ane, and cadinane skeletons. The two Clade IV putative sesquiterpene synthases, Fla10 and Fla11, are clustered most closely with cuprenene synthases Cop6, Fompi1, and Sh 159379. The cuprenenes could be further transformed into diverse sesquiterpenoids with *seco*-cuparane and cuparane skeletons by subsequent modification. Other putative sesquiterpene synthases in Clade III may be responsible for the biosynthesis of sesquiterpenoids with sterpurane, isolactarane and cucumane skeletons by 1,11-cyclization mechanism. In this report, four more types of sesquiterpene derived from 1,6- and 1,10-cyclization including nor-eudesmane, spiroaxane, cadinane, and *seco*-cuparane were identified for the first time in the mycelia culture of *F. velutipes*. These findings confirm that *F. velutipes* possesses a number of as of yet uncharacterized sesquiterpene synthases that follow 1,6-, 1,10-, and 1,11-cyclization mechanisms.

Identification of these sesquiterpenes and prediction of the corresponding sesquiterpene synthases enables us to propose the biogenetic network for sesquiterpenes in *F. velutipes* as presented in Scheme 1. To elucidate the mechanisms of cyclization and terpene synthases-skeleton relationship, inactivation or heterologous expression of sesquiterpene synthase genes in the genome of *F. velutipes* are required.

In conclusion, 15 new sesquiterpenes with five different skeletons and two new ergosterol derivatives were identified from the culture of *F. velutipes*. To the best of our knowledge, the isolation of flammufuranones A (1) and B (2) represented the first instance of *seco*-cuparane sesquiterpenoids. The biogenetic pathway for sesquiterpenes with various frameworks in *F. velutipes* was proposed on the basis of genome sequence analysis and chemical work on this fungus. Preliminary bioassay results suggested that some of the new sesquiterpenes had moderate inhibitions against DPP-4 and HMG-CoA reductase, which provided evidence for the future application of *F. velutipes* as functional food. The mushroom *F. velutipes* can serve as an ideal model to investigate the sesquiterpenoid biosynthesis in basidiomycota due to the presence of sesquiterpene synthase in clades I–IV and the production of the corresponding secondary metabolites.

EXPERIMENTAL SECTION

General Experimental Procedures. Optical rotations were measured on a polarimeter with sodium light (589 nm). UV spectra were obtained on a UV–vis spectrophotometer. ^1H and ^{13}C (^1H -decoupled) NMR data were acquired by using TMS as an internal standard. The HSQC and HMBC experiments were optimized for 145.0 and 8.0 Hz, respectively. The 1D and 2D NMR spectra were performed using standard software. Semipreparative HPLC was performed on a system using an ODS column (C18, 250 × 9.4 mm, 5 μm ; detector: UV) with a flow rate of 2.5 mL/min.

Fungal Material. The fungal strain *F. velutipes* was isolated from the fruiting bodies collected in the Yunnan-Guizhou plateau and was identified by ITS1-ITS2 sequence with the accession number KP867925 in GenBank.

Fermentation and Extraction. *F. velutipes* was cultured on slant of potato dextrose agar at 25 °C for 14 days. Agar plugs were inoculated in a 500 mL Erlenmeyer flask containing 150 mL of potato dextrose broth with the final pH of 6.5 before sterilization, and incubated at 25 °C on a rotary shaker at 180 rpm for 1 week. Large scale fermentation was carried out in 20 500 mL flasks each containing 80 g of rice and 120 mL of distilled water. Each flask was inoculated with 5.0 mL of the culture medium and incubated at 25 °C for 40 days. The fermented rice substrate was extracted repeatedly with ethyl acetate (3 × 3L) at room temperature. The organic solvent was evaporated under vacuum to afford the crude extract (16.2 g).

Isolation and Characterization Data. The EtOAc extract was subjected to silica gel column chromatography eluted with a gradient of *n*-hexane-ethyl acetate (v/v 100:0, 100:1, 50:1, 20:1, 10:1, 5:1), followed by dichloromethane-methanol (200:0, 200:1, 100:1, 80:1, 50:1, 30:1, 20:1, 15:1, 10:1, 5:1, 0:1) to give 16 fractions (fractions 1–16) on the basis of TLC. Fr. 7 (665.8 mg) was first separated on ODS column chromatography eluted with MeOH–H₂O in gradient eluent (10:90, 20:80, 30:70, 40:60, 50:50, 60:40, 70:30, 80:20, 100:0) to give nine subfractions (fr. 7.1–7.9). Fr. 7.6 (90.1 mg) was further subjected to Sephadex LH-20 eluted with MeOH to give seven subfractions (fr. 7.6.1–7.6.7). Fr. 7.6.4 (47.3 mg) was further purified by RP-HPLC using 25% acetonitrile in water to afford 4 (5.74 mg, t_{R} 17.6 min), 15 (2.75 mg, t_{R} 25.2 min), 16 (2.74 mg, t_{R} 25.9 min). Fr. 8 (208.0 mg) was subject to Sephadex LH-20 eluted with MeOH to give eight subfractions (fr. 8.1–8.8). Fr. 8.5 (29.7 mg) was further purified by RP-HPLC using 30% acetonitrile in water to obtain 5 (21.1 mg, t_{R} 24.7 min). Fr. 9 (240.0 mg) was separated on ODS column chromatography eluted with MeOH–H₂O in gradient eluent (10:90, 15:85, 20:80, 25:75, 30:70, 50:50, 100:0) to afford 3 (56.7 mg, t_{R} 13.3 min). Fr. Ten (380.0 mg) was separated on ODS column chromatography eluted with MeOH–H₂O in gradient eluent (10:90, 15:85, 20:80, 25:75, 30:70, 50:50, 75:25, 100:0) to afford 9 (102.9 mg, t_{R} 20.8 min). Fr. 11 (1.1 g) was subjected to Sephadex LH-20 eluted with MeOH to yield eight subfractions (fr. 11.1–11.8). Fr. 11.5 was further purified by RP-HPLC using 35% acetonitrile in water to obtain 17 (1.9 mg, t_{R} 30.1 min), 18 (1.7 mg, t_{R} 31.1 min). Fr. 12 (859.8 mg)

was separated on ODS column chromatography eluted with MeOH–H₂O in gradient eluent (10:90, 15:85, 20:80, 25:75, 30:70, 40:60, 50:50, 75:25, 100:0) to give ten subfractions. Fr. 12.5 (174.2 mg) was further purified by RP-HPLC using 17% acetonitrile in water to obtain 7 (13.6 mg, t_{R} 14.8 min), 11 (51.1 mg, t_{R} 13.3 min), 6 (3.2 mg, t_{R} 14.3 min), 14 (13.9 mg, t_{R} 15.4 min). Fr. 12.6 (94.3 mg) was further purified by RP-HPLC using 18% acetonitrile in water to obtain 10 (2.73 mg, t_{R} 12.1 min), 8 (8.6 mg, t_{R} 17.3 min), 13 (3.0 mg, t_{R} 16.3 min). Fr. 13 (361.7 mg) was also subjected to ODS column chromatography eluted with MeOH–H₂O (10:90, 15:85, 20:80, 25:75, 30:70, 40:60, 50:50, 75:25, 100:0) in gradient eluent to obtain eight subfractions (fr. 13.1–13.8). Fr. 13.5 (37.4 mg) was further purified by RP-HPLC using 20% acetonitrile in water to afford 1 (3.5 mg, t_{R} 19.8 min), 2 (8.5 mg, t_{R} 20.0 min), 12 (1.4 mg, t_{R} 18.0 min).

Flammufuranone A (1). Colorless oil; $[\alpha]_{\text{D}}^{25} + 44.99$ (c 1.0 methanol); CD (c 1.08×10^{-3} M, methanol) λ_{max} ($\Delta\epsilon$) 228 (–3.09), 295 (+3.11), 340 (–0.56); UV (methanol) λ_{max} nm (log ϵ) 263 (3.2); IR (neat) ν_{max} 2977, 1708, 1580, 1454, 1391, 1376, 1357, 1174, 1107 cm^{-1} ; positive HRTOFMS m/z $[\text{M}+\text{H}]^+$ 279.1227 (calcd for C₁₅H₁₉O₅, 279.1227); ^1H and ^{13}C NMR spectroscopic data see in Table 1.

Flammufuranone B(2). Colorless oil; $[\alpha]_{\text{D}}^{25} + 14.00$ (c 1.0 methanol); CD (c 1.08×10^{-3} M, methanol) λ_{max} ($\Delta\epsilon$) 216 (–6.58), 263 (+14.54), 300 (–4.82); UV (methanol) λ_{max} nm (log ϵ) 263 (3.2); IR (neat) ν_{max} 2978, 1707, 1583, 1454, 1381, 1361, 1180, 1108 cm^{-1} ; positive HRTOFMS m/z $[\text{M}+\text{H}]^+$ 279.1227 (calcd for C₁₅H₁₉O₅, 279.1227); ^1H and ^{13}C NMR spectroscopic data see in Table 1.

Flammuspironone A (3). Colorless needles; mp dec 181–183 °C; $[\alpha]_{\text{D}}^{25} + 12.00$ (c 1.0 methanol); CD (c 1.12×10^{-3} M, methanol) λ_{max} ($\Delta\epsilon$) 208 (–6.78), 241 (+1.62), 281 (+0.07), 319 (+0.44); UV (methanol) λ_{max} nm (log ϵ) 237 (3.2); IR (neat) ν_{max} 3412, 2963, 2922, 1693, 1635, 1461, 1379, 1299, 1210, 1150 cm^{-1} ; positive HRTOFMS m/z $[\text{M}+\text{Na}]^+$ 291.1571 (calcd for C₁₅H₂₄O₄Na, 291.1567); ^1H NMR spectroscopic data see in Table 2 and ^{13}C NMR data see in Table 3.

Flammuspironone B (4). Colorless oil; $[\alpha]_{\text{D}}^{25} + 4.00$ (c 1.0 methanol); CD (c 1.19×10^{-3} M, methanol) λ_{max} ($\Delta\epsilon$) 208 (–6.73), 246 (+0.57), 280 (–0.05), 320 (+0.32); UV (methanol) λ_{max} nm (log ϵ) 237 (3.2); IR (neat) ν_{max} 3400, 2958, 2930, 1693, 1636, 1459, 1381, 1336, 1163 cm^{-1} ; positive HRTOFMS m/z $[\text{M}+\text{H}]^+$ 253.1798 (calcd for C₁₅H₂₅O₃, 253.1798); ^1H NMR spectroscopic data see in Table 2 and ^{13}C NMR data see in Table 3.

Flammuspironone C (5). Colorless oil; $[\alpha]_{\text{D}}^{25} - 22.00$ (c 1.0 methanol); CD (c 1.19×10^{-3} M, methanol) λ_{max} ($\Delta\epsilon$) 210 (–2.76), 254 (+0.21), 276 (+0.08), 319 (+0.56); UV (methanol) λ_{max} nm (log ϵ) 237 (3.2); IR (neat) ν_{max} 3390, 2955, 1698, 1636, 1459, 1380, 1268, 1205, 1175 cm^{-1} ; positive HRTOFMS m/z $[\text{M}+\text{H}]^+$ 253.1796 (calcd for C₁₅H₂₅O₃, 253.1798); ^1H NMR spectroscopic data see in Table 2 and ^{13}C NMR data see in Table 3.

Flammuspironone D(6). Colorless oil; $[\alpha]_{\text{D}}^{25} - 12.00$ (c 1.0 methanol); CD (c 1.12×10^{-3} M, methanol) λ_{max} ($\Delta\epsilon$) 206 (–3.87), 246 (+1.08), 281 (+0.13), 320 (+0.54); UV (methanol) λ_{max} nm (log ϵ) 240 (3.3); IR (neat) ν_{max} 3360, 2944, 1697, 1649, 1454, 1253, 1203, 1037 cm^{-1} ; positive HRTOFMS m/z $[\text{M}+\text{H}]^+$ 269.1747 (calcd for C₁₅H₂₅O₄, 269.1747); ^1H NMR spectroscopic data see in Table 2 and ^{13}C NMR data see in Table 3.

Flammuspironone E (7). Colorless oil; $[\alpha]_{\text{D}}^{25} - 27.00$ (c 1.0 methanol); CD (c 1.12×10^{-3} M, methanol) λ_{max} ($\Delta\epsilon$) 214 (–3.46), 252 (+0.49), 285 (+0.06), 323 (+0.44); UV (methanol) λ_{max} nm (log ϵ) 236 (3.1); IR (neat) ν_{max} 3355, 2954, 1697, 1649, 1457, 1267, 1174 cm^{-1} ; positive HRTOFMS m/z $[\text{M}+\text{Na}]^+$ 291.1568 (calcd for C₁₅H₂₄O₄Na, 291.1567); ^1H NMR spectroscopic data see in Table 2 and ^{13}C NMR data see in Table 3.

Flammuspironone F (8). Colorless oil; $[\alpha]_{\text{D}}^{25} - 6.00$ (c 1.0 methanol); CD (c 1.12×10^{-3} M, methanol) λ_{max} ($\Delta\epsilon$) 210 (–1.56), 258 (+0.15), 274 (+0.11), 319 (+0.52); UV (methanol) λ_{max} nm (log ϵ) 237 (3.2); IR (neat) ν_{max} 3355, 2942, 2832, 1692, 1649, 1454, 1255, 1112, 1028 cm^{-1} ; positive HRTOFMS m/z $[\text{M}+\text{Na}]^+$ 269.1747 (calcd for

$C_{15}H_{25}O_4$, 269.1747); 1H NMR spectroscopic data see in Table 2 and ^{13}C NMR data see in Table 3.

Flammuspiron G (9). Colorless needles; mp dec 186–188 °C; $[\alpha]_D^{25}$ –1.00 (c 1.0 methanol); CD (c 1.19×10^{-3} M, methanol) λ_{max} ($\Delta\epsilon$) 231 (–3.11), 279 (+0.04), 323 (+0.24); UV (methanol) λ_{max} nm (log ϵ) 236 (3.1); IR (neat) ν_{max} 3298, 2956, 1715, 1698, 1637, 1463, 1369, 1272, 1209, 1131 cm^{-1} ; positive HRTOFMS m/z $[M+Na]^+$ 275.1617 (calcd for $C_{15}H_{24}O_3Na$, 275.1618); ^{13}C NMR spectroscopic data see in Table 3 and 1H NMR data see in Table 4.

Flammuspiron H (10). Colorless needles; mp dec 146–148 °C; $[\alpha]_D^{25}$ +7.00 (c 1.0 methanol); CD (c 1.12×10^{-3} M, methanol) λ_{max} ($\Delta\epsilon$) 237 (+2.55), 283 (+0.08), 326 (+0.25); UV (methanol) λ_{max} nm (log ϵ) 234 (3.0); IR (neat) ν_{max} 3355, 2942, 2832, 1692, 1649, 1454, 1255, 1112, 1028 cm^{-1} ; positive HRTOFMS m/z $[M+Na]^+$ 291.1567 (calcd for $C_{15}H_{24}O_4Na$, 291.1567); ^{13}C NMR spectroscopic data see in Table 3 and 1H NMR data see in Table 4.

Flammuspiron I (11). Colorless needles; mp dec 189–191 °C; $[\alpha]_D^{25}$ –1.00 (c 1.0 methanol); CD (c 1.12×10^{-3} M, methanol) λ_{max} ($\Delta\epsilon$) 232 (+3.18), 278 (+0.07), 320 (+0.33); UV (methanol) λ_{max} nm (log ϵ) 234 (3.0); IR (neat) ν_{max} 3368, 2972, 1695, 1634, 1449, 1379, 1270, 1202, 1143 cm^{-1} ; positive HRTOFMS m/z $[M+H]^+$ 269.1749 (calcd for $C_{15}H_{25}O_4$, 269.1747); ^{13}C NMR spectroscopic data see in Table 3 and 1H NMR data see in Table 4.

Flammuspiron J (12). Colorless needles; mp dec 187–189 °C; $[\alpha]_D^{25}$ –21.00 (c 1.0 methanol); CD (c 1.20×10^{-3} M, methanol) λ_{max} ($\Delta\epsilon$) 219 (+0.90), 241 (–0.32), 321 (+0.38); UV (methanol) λ_{max} nm (log ϵ) 235 (3.1); IR (neat) ν_{max} 3345, 2926, 2852, 1694, 1649, 1454, 1376, 1110, 1027 cm^{-1} ; positive HRTOFMS m/z $[M+H]^+$ 251.1642 (calcd for $C_{15}H_{23}O_3$, 251.1642); ^{13}C NMR spectroscopic data see in Table 3 and 1H NMR data see in Table 4.

7,13,14-Trihydroxy-4-cadinen-15-oic Acid Methyl Ester (13). Colorless oil; $[\alpha]_D^{25}$ –10.00 (c 1.0 methanol); CD (c 1.01×10^{-3} M, methanol) λ_{max} ($\Delta\epsilon$) 224 (–0.24), 250 (+0.82), 296 (–0.07); UV (methanol) λ_{max} nm (log ϵ) 223 (3.1); IR (neat) ν_{max} 3363, 2945, 2878, 1714, 1649, 1434, 1271, 1081 cm^{-1} ; positive HRTOFMS m/z $[M+H]^+$ 299.1852 (calcd for $C_{16}H_{27}O_5$, 299.1853); ^{13}C NMR spectroscopic data see in Table 3 and 1H NMR data see in Table 4.

1,2,6,10-Tetrahydroxy-3,9-epoxy-14-nor-5(15)-eudesmane (14). Colorless oil; $[\alpha]_D^{25}$ –98.98 (c 1.0 methanol); CD (c 1.11×10^{-3} M, methanol) λ_{max} ($\Delta\epsilon$) 211 (–7.68), 236 (+0.34); UV (methanol) λ_{max} nm (log ϵ) 203 (3.0); IR (neat) ν_{max} 3362, 2955, 1649, 1454, 1235, 1143, 1083 cm^{-1} ; positive HRTOFMS m/z $[M+Na]^+$ 293.1359 (calcd for $C_{14}H_{22}O_5Na$, 293.1359); ^{13}C NMR spectroscopic data see in Table 3 and 1H NMR data see in Table 4.

Flamvelutpenoid E (15).¹⁸ White powder; 196–198 °C; $[\alpha]_D^{25}$ –29.00 (c 1.0 methanol); CD (c 1.21×10^{-3} M, methanol) λ_{max} ($\Delta\epsilon$) 210 (+0.56), 240 (–1.74), 279 (+0.08); UV (methanol) λ_{max} nm (log ϵ) 241 (3.0); IR (neat) ν_{max} 3370, 2960, 1689, 1609, 1410, 1378, 1275, 1190, 1130 cm^{-1} ; positive HRTOFMS m/z $[M+H]^+$ 249.1485 (calcd for $C_{15}H_{21}O_3$, 249.1485); 1H and ^{13}C NMR spectroscopic data see in Table 5.

Flamvelutpenoid F (16). Colorless oil; $[\alpha]_D^{25}$ –20.00 (c 1.0 methanol); CD (c 1.21×10^{-3} M, methanol) λ_{max} ($\Delta\epsilon$) 216 (–0.68), 238 (–1.37); UV (methanol) λ_{max} nm (log ϵ) 240 (3.0); IR (neat) ν_{max} 3399, 2960, 1697, 1610, 1413, 1378, 1273, 1190, 1128 cm^{-1} ; positive HRTOFMS m/z $[M+H]^+$ 249.1485 (calcd for $C_{15}H_{21}O_3$, 249.1485); 1H and ^{13}C NMR spectroscopic data see in Table 5.

3,9,25-Trihydroxy-24-hydroxymethylergosta-7,22-dien-6-one (17). white powder; 231–234 °C; $[\alpha]_D^{25}$ –20.00 (c 1.0 methanol); CD (c 0.65×10^{-3} M, methanol) λ_{max} ($\Delta\epsilon$) 249 (–8.56), 329 (+2.27); UV (methanol) λ_{max} nm (log ϵ) 239 (3.0); IR (neat) ν_{max} 3358, 2940, 1673, 1458, 1372, 1301, 1251, 1135, 1108 cm^{-1} ; positive HRTOFMS m/z $[M+Na]^+$ 483.3081 (calcd for $C_{28}H_{44}O_5Na$, 483.3081); 1H NMR (500 MHz, CD_3OD) δ_H 5.59 (d, J = 1.8 Hz, H-7), 5.43 (dd, J = 15.3, 8.6 Hz, H-22), 5.28 (dd, J = 15.3, 9.3 Hz, H-23), 4.08 (m, H-3), 3.85 (dd, J = 10.6, 6.3 Hz, H-28a), 3.60 (dd, J = 10.6, 6.9 Hz, H-28b), 3.29 (o, H-5), 2.65 (m, H-14), 2.37 (td, J = 13.6, 4.2 Hz, H-1a), 2.21 (o, H-24), 2.16 (o, H-20), 2.05 (o, H-11a), 1.98 (o, H-12a), 1.91 (o, H-16a), 1.89 (o, H-2a), 1.79 (m, H-11b), 1.78 (o, H-12b), 1.70 (o, H-2b), 1.64

(o, H-15a), 1.63 (o, H-4a), 1.54 (o, H-15b), 1.49 (o, H-17), 1.47 (o, H-16b), 1.45 (o, H-4b), 1.21 (o, H-1b), 1.19 (s, H-27), 1.16 (s, H-26), 1.10 (d, J = 6.6 Hz, H-21), 0.96 (s, H-19), 0.70 (s, H-18); ^{13}C NMR (125 MHz, CD_3OD) δ_C 204.2 (C-6), 164.2 (C-8), 141.3 (C-22), 127.4 (C-23), 124.1 (C-7), 74.8 (C-9), 73.6 (C-25), 65.8 (C-3), 64.1 (C-28), 57.3 (C-17), 56.4 (C-24), 53.1 (C-14), 45.9 (C-13), 43.6 (C-10), 43.0 (C-5), 41.7 (C-20), 36.6 (C-12), 29.7 (C-27), 29.0 (C-11), 28.8 (C-16), 28.7 (C-4), 28.4 (C-2), 26.0 (C-26), 25.7 (C-1), 23.5 (C-15), 21.2 (C-21), 16.5 (C-19), 12.6 (C-18).

3,14,25-Trihydroxy-24-hydroxymethylergosta-7,22-dien-6-one (18). white powder; 254–257 °C; $[\alpha]_D^{25}$ +33.99 (c 1.0 methanol); CD (c 0.65×10^{-3} M, methanol) λ_{max} ($\Delta\epsilon$) 248 (–4.46), 328 (+2.03); UV (methanol) λ_{max} nm (log ϵ) 241 (3.0); IR (neat) ν_{max} 3365, 2937, 1666, 1455, 1379, 1204, 1186, 1143, 1036 cm^{-1} ; positive HRTOFMS m/z $[M + Na]^+$ 483.3081 (calcd for $C_{28}H_{44}O_5Na$, 483.3081); 1H NMR (500 MHz, CD_3OD) δ_H 5.84 (d, J = 2.6 Hz, H-7), 5.45 (dd, J = 15.2, 8.5 Hz, H-22), 5.29 (dd, J = 15.2, 9.3 Hz, H-23), 4.11 (br s, H-3), 3.85 (dd, J = 10.6, 6.4 Hz, H-28a), 3.60 (dd, J = 10.6, 6.9 Hz, H-28b), 2.85 (m, H-9), 2.74 (dd, J = 12.2, 3.7 Hz, H-5), 2.18 (o, H-24), 2.17 (o, H-20), 2.11 (o, H-12a), 1.99 (o, H-17), 1.95 (o, H-2a), 1.90 (o, H-16a), 1.89 (o, H-4a), 1.79 (o, H-1a), 1.78 (o, H-15a), 1.71 (o, H-12b), 1.63 (o, H-11a), 1.62 (o, H-2b), 1.60 (o, H-11b), 1.59 (o, H-15b), 1.56 (o, H-1b), 1.55 (o, H-4b), 1.41 (o, H-16b), 1.19 (s, H-27), 1.17 (s, H-26), 1.07 (d, J = 6.6 Hz, H-21), 0.87 (s, H-19), 0.74 (s, H-18); ^{13}C NMR (125 MHz, CD_3OD) δ_C 204.9 (C-6), 166.3 (C-8), 141.7 (C-22), 127.2 (C-23), 123.4 (C-7), 85.4 (C-14), 73.7 (C-25), 66.0 (C-3), 64.2 (C-28), 56.4 (C-24), 51.6 (C-17), 49.6 (C-5), 47.6 (C-13), 47.5 (C-9), 41.3 (C-20), 40.1 (C-10), 32.8 (C-1), 32.0 (C-4), 31.8 (C-12), 29.7 (C-27), 28.5 (C-2), 28.5 (C-11), 27.8 (C-16), 25.9 (C-26), 21.4 (C-15), 21.3 (C-21), 16.6 (C-18), 12.5 (C-19).

X-ray Crystallographic Analysis of Flammuspiron A (3). X-ray diffraction data collection was carried out from a $0.38 \times 0.38 \times 0.38$ mm³ crystal with an Eos CCD using graphite-monochromated Cu K_{α} radiation (λ = 1.54180 Å at 108.0 K). The structure was solved by direct methods (SHELXS-97) and refined using full-matrix least-squares difference Fourier techniques. Crystal data of 3: $C_{15}H_{24}O_4$, MW 268.34, space group monoclinic, $P2_12_12_1$; unit cell dimensions a = 7.0162(4) Å, b = 9.8847(6) Å, c = 20.6163(13) Å, α = 90.00°, β = 90.00°, γ = 90.00°, V = 1429.80(11) Å³, Z = 4, D_{calc} = 1.247 mg/m³, μ = 0.722 mm^{–1}, $F(000)$ = 584.0. A total of 4452 reflections were measured, in which 2684 unique ($|F|^2 \geq 2\sigma(F)^2$) were used in all calculations. Crystallographic data (excluding structure factors) for 3 have been deposited in the Cambridge Crystallographic Data Centre: CCDC reference number 1487771. These data can be obtained, free of charge, from Cambridge Crystallographic Data Centre via http://www.ccdc.cam.ac.uk/data_request/cif.

Computation Section. Systematic conformational analysis of 1a and 2a was carried out by using the MMFF94 molecular mechanics force field. All MMFF minima were reoptimized with DFT calculations at the B3LYP/6-311G(d,p) level using the Gaussian09 program. The geometry was optimized starting from various initial conformations, with vibrational frequency calculations confirming the presence of minima. The 40 lowest electronic transitions were calculated using time-dependent density-functional theory (TDDFT) methodology at the B3LYP/6-311G(d,p) level. ECD spectra were stimulated using a Gaussian function with a half-bandwidth of 0.35 and 0.40 eV, respectively. The overall ECD spectra were then generated according to Boltzmann weighting of each conformer.

Cell Proliferation Assays. MTT cell proliferation assays using the A549, K562, H460, and HepG2 cell line were performed as previously described.¹¹

Assay for Aldose Reductase.²³ Rat lenses were obtained from the eyes of 8-week-old Sprague–Dawley rats weighing 250–280 g. The incubation mixture (1.0 mL in total) contained 135 mM Na/K phosphate buffer (pH 7.0), 100 mM Li_2SO_4 , 0.03 mM NADPH, 1 mM DL-glyceraldehyde as a substrate, and an enzyme fraction (50 μ L), with or without the sample solution (25 μ L). The reaction was initiated by the addition of NADPH at 37 °C and terminated by the addition of 0.5 M aqueous HCl (0.3 mL). In order to convert NADP to a fluorescent product, a 6 M aqueous NaOH solution containing 10 mM

1H-imidazole (1 mL) was added, and the mixture was heated to 60 °C for 10 min. The fluorescence was measured with a spectrofluorometric detector (BioTek, Synergy HT) at excitation and emission wavelengths of 360 and 460 nm, respectively. The RLAR assays were performed in triplicate to yield measures of the SE. The concentration of each test sample giving rise to 50% inhibition of activity (IC_{50}) was estimated from the least-squares regression line of the logarithmic concentration plotted against the remaining activity.

Inhibition Assay against HMG-CoA Reductase. The HMG-CoA reductase prepared from pig liver microsomes was tested by the previously described colorimetric method with a slight modification.²⁴ The blank was prepared by adding potassium phosphate buffer instead of HMG-CoA reductase. The control was prepared by adding potassium phosphate buffer instead of test compounds. The inhibition rates (%) = $[(OD_{\text{test}} - OD_{\text{test blank}}) - (OD_{\text{control blank}} - OD_{\text{control}})] / (OD_{\text{control blank}} - OD_{\text{control}}) \times 100\%$.

Assay for DPP-4 Inhibitory Activity.²⁵ A mixture containing 100 μL of tris(hydroxymethyl)aminomethane/maleic acid buffer solution (0.1 M, pH 7.2), 25 μL of 3.2 mM Gly-Pro-4-naphthylamide (Bachem, Switzerland), and 50 μL of sample solution was incubated at 37 °C for 10 min, and then 25 μL of DPP-IV solution was added into the solution. The mixture was incubated at 37 °C for 1 h. The reaction was terminated by adding a solution (100 μL) of 0.2% Fast Garnet GBC salt (Sigma) in 0.5 M sodium citrate buffer solution (pH 3.78) including 10% polyoxyethylene sorbitanmonolaurate (Wako, Japan). The assay was conducted in a 96-well plate and the absorbance was measured at 405 nm (value *a*). Simultaneously, the absorbance of the reaction mixture without any sample solution was measured (value *b*). Moreover, the absorbance of the reaction mixture without the DPP-IV solution was measured, respectively (value *ac* and value *bc*). The DPP-IV inhibitory rate (%) was calculated by $[(b - bc) - (a - ac)] / (b - bc) \times 100$. From the inhibitory curve, taking inhibitory rate (%) at various concentrations of the compound on the ordinate and the logarithm of concentrations of the compound on the abscissa, the concentration for 50% inhibition was obtained. In all cases, a linear relation was observed between 20% and 80% inhibition. Then, each average was shown as the IC_{50} value of each compound.

Homology Searches and Phylogenetic Tree Construction. The 19 fungal sesquiterpene synthases previously identified from *C. cinereus*, *O. olearius*, and *S. hirsutum* used with the NCBI BLAST software to perform homology searches of the *F. velutipes* assembly. Gene structures were prediction by Augustus using *Laccaria bicolor* as reference. Upon identification of putative sesquiterpene synthase amino acid sequences in *F. velutipes*, alignments were computed using ClustalW and phylogenetic analyses were conducted using MEGA version 7.0 using the default parameters for the Neighbor-Joining method with a bootstrap test of phylogeny (1000 replicates). Alignments were manually refined by removing sesquiterpene synthase sequences that did not contain both of the well conserved metal-binding motifs characteristic for sesquiterpene synthases showed clear mistakes in splicing predictions, or were not a characteristic length (250–425 amino acids) for this class of enzymes

■ ASSOCIATED CONTENT

Supporting Information

The Supporting Information is available free of charge on the ACS Publications website at DOI: 10.1021/acs.joc.6b01971.

NMR spectra for compounds 1–18 (PDF)

X-ray crystallographic data of 3 (CIF)

■ AUTHOR INFORMATION

Corresponding Author

*Tel: +86 10 64806074; E-mail: liuhw@im.ac.cn.

Author Contributions

#Q.T., K.M., and Y.Y. contributed equally to this work.

Notes

The authors declare no competing financial interest.

■ ACKNOWLEDGMENTS

Financial supports of the National Nature Science Foundation (21472233), the Ministry of Science and Technology of China (2014CB138304), the National Basic Research Program of China (973 Program, 2014CB138305), and the Youth Innovation Promotion Association of Chinese Academy of Sciences (2014074) are acknowledged. Dr. Wenzhao Wang (State Key Laboratory of Mycology, Institute of Microbiology, Chinese Academy of Sciences) is appreciated for their help in measuring MS data.

■ REFERENCES

- (1) Fraga, B. M. *Nat. Prod. Rep.* **2013**, *30*, 1226–1264.
- (2) Maimone, T. J.; Baran, P. S. *Nat. Chem. Biol.* **2007**, *3*, 396–407.
- (3) Jiao, L.; Yu, Z. X. *J. Org. Chem.* **2013**, *78*, 6842–6848.
- (4) Spittler, P. *Chem. - Eur. J.* **2008**, *14*, 9100–9110.
- (5) Huang, M.; Sanchez-Moreiras, A. M.; Abel, C.; Sohrabi, R.; Lee, S.; Gershenzon, J.; Tholl, D. *New Phytol.* **2012**, *193*, 997–1008.
- (6) Quin, M. B.; Flynn, C. M.; Schmidt-Dannert, C. *Nat. Prod. Rep.* **2014**, *31*, 1449–1473.
- (7) Hou, L. F.; Huang, H. C. *Pharmacol. Ther.* **2016**, *166*, 123.
- (8) Shu, Y. Z. *J. Nat. Prod.* **1998**, *61*, 1053–1071.
- (9) Wang, Y. Q.; Bao, L.; Yang, X. L.; Dai, H. Q.; Guo, H.; Yao, X. S.; Zhang, L. X.; Liu, H. W. *Helv. Chim. Acta* **2012**, *95*, 261–267.
- (10) Wang, Y. Q.; Bao, L.; Yang, X. L.; Li, L.; Li, S. F.; Gao, H.; Yao, X. S.; Wen, H. A.; Liu, H. W. *Food Chem.* **2012**, *132*, 1346–1353.
- (11) Wang, Y. Q.; Bao, L.; Liu, D. L.; Yang, X. L.; Li, S. F.; Gao, H.; Yao, X. S.; Wen, H. A.; Liu, H. W. *Tetrahedron* **2012**, *68*, 3012–3018.
- (12) Wawrzyn, G. T.; Quin, M. B.; Choudhary, S.; López-Gallego, F.; Schmidt-Dannert, C. *Chem. Biol.* **2012**, *19*, 772–783.
- (13) Quin, M. B.; Flynn, C. M.; Wawrzyn, G. T.; Choudhary, S.; Schmidt-Dannert, C. *ChemBioChem* **2013**, *14*, 2480–2491.
- (14) Park, Y. J.; Baek, J. H.; Lee, S.; Kim, C.; Rhee, H.; Kim, H.; Seo, J. S.; Park, H. R.; Yoon, D. E.; Nam, J. Y.; Kim, H. I.; Kim, J. G.; Yoon, H.; Kang, H. W.; Cho, J. Y.; Song, E. S.; Sung, G. H.; Yoo, Y. B.; Lee, C. S.; Lee, B. M.; Kong, W. S. *PLoS One* **2014**, *9*, e93560.
- (15) Ma, K.; Ren, J. W.; Han, J. J.; Bao, L.; Li, L.; Yao, Y. J.; Sun, C.; Zhou, B.; Liu, H. W. *J. Nat. Prod.* **2014**, *77*, 1847–1852.
- (16) Frelek, J.; Pakulski, Z.; Zamojski, A. *Tetrahedron: Asymmetry* **1996**, *7*, 1363–1372.
- (17) Scott, A. I.; Wrixon, A. D. *Tetrahedron* **1970**, *26*, 3695–3715.
- (18) Bai, J.; Chen, H.; Fang, Z. F.; Yu, S. S.; Ma, S. G.; Li, Y.; Qu, J.; Xu, S.; Ren, J. H.; Lü, H. N.; Chen, X. *J. Asian Nat. Prod. Res.* **2012**, *14*, 940–949.
- (19) Riccio, R.; Santaniello, M.; Greco, O. S.; Minale, L. *J. Chem. Soc., Perkin Trans. 1* **1989**, 823–826.
- (20) Wu, X. L.; Lin, S.; Zhu, C. G.; Yue, Z. G.; Yu, Y.; Zhao, F.; Liu, B.; Dai, J. G.; Shi, J. G. *J. Nat. Prod.* **2010**, *73*, 1294–1300.
- (21) De Silva, D. D.; Rapior, S.; Hyde, K. D.; Bahkali, A. H. *Fungal Divers.* **2012**, *56*, 1–29.
- (22) Bisen, P. S.; Baghel, R. K.; Sanodiya, B. S.; Thakur, G. S.; Prasad, G. B. K. S. *Curr. Med. Chem.* **2010**, *17*, 2419–2430.
- (23) Hong, Y. J.; Tantillo, D. J. *J. Am. Chem. Soc.* **2014**, *136*, 2450–2463.
- (24) Wang, K.; Bao, L.; Xiong, W. P.; Ma, K.; Han, J. J.; Wang, W. Z.; Yin, W. B.; Liu, H. W. *J. Nat. Prod.* **2015**, *78*, 1977–1989.
- (25) Abe, M.; Akiyama, T.; Nakamura, H.; Kojima, F.; Harada, S.; Muraoka, Y. *J. Nat. Prod.* **2004**, *67*, 999–1004.